

Model and Numerical Simulations of Vehicle Platform Stabilization

D. S. Cameron[†], J. C. Chipman[‡], N. Kheir[†] and M. Shillor[‡],

[†]Department of Electrical Engineering,
[‡]Department of Mathematics and Statistics,
Oakland University,
Rochester, Michigan 48309,

October 26, 2001

Abstract

A new model for the stabilization of an automotive platform with a low power active suspension is presented, analyzed and numerically simulated. The model consists of a nonlinear coupled system of three ordinary differential equations. The nonlinearity arises from a spring-like device with negative spring constant, which is the heart of the new approach. The problem may have one or three steady states. The system is numerically simulated and the results presented and analyzed. The problem of control of the system by a displacement actuator is left open.

Keywords: Vehicle platform stabilization, nonlinear dynamical system, negative spring constant.

1 Introduction

The design of active controls of vehicle suspensions has been investigated (see, e.g., [9, 11]) aiming at increasing their performance. Various forms of active suspensions for platform stabilization have been proposed and investigated in [3, 4, 7, 9, 11, 12]. Currently, a typical mechanization of vehicle active suspension requires a significant external power supply, which is a considerable burden on the engine. This power drain increases the fuel consumption of the vehicle, which is contrary to current fuel economy regulations and automotive manufacturing trends world-wide. The goal of the new approach to vehicle platform stabilization is to reduce the significant power required for operation of current active suspension systems.

The novel approach adopted here, proposed first by Cameron [6], for a low power active suspension addresses this very issue of energy consumption of the

system. The novelty lies in the low energy consumption which is achieved by the interaction between a linear and a highly nonlinear spring, connected in series. In the operating displacement range of the suspension system the nonlinear spring behaves as a spring with negative stiffness, while supporting a positive load.

In this paper, the model which is in the form of a system of three differential equations is presented. One of the equations contains the nonlinear spring with a negative stiffness, similar to the so-called “Duffing Oscillator.” The system is found to have one or three steady states. Then, the model is simulated numerically. Typical types of behavior, and the approach to the steady states are depicted, and the stability of the the steady solutions investigated. Related results for a system which includes the nonlinear spring and friction have been obtained in [10]. The control aspects of the model, via a displacements actuator, will be investigated in the near future. The purpose here is to gain insight into the possible types of behavior of this model for the suspension.

The model is presented in Section 2, where the assumptions underlying it are explained, and the nonlinear spring, the so-called Vertically Compressed Horizontally Sliding Spring ([10]) described. The system energy is derived and a number of conclusions drawn. The system’s steady states are investigated in Section 3, where it is shown that the nonlinear spring system can have one or three steady state solutions. It seems that in the case with three steady solution, the zero solution is unstable and the other two are stable; in the case of a single (zero) solution it is stable. This is based on the results of the numerical simulations of the model described in Section 4, and is similar to the behavior of the Duffing Oscillator. The numerical scheme, which is based on Euler discretization, is presented and a number of typical or interesting simulations depicted. The results are summarized in section 5, where some additional problems are posed and future research indicated.

2 The model

In this section the model of a vehicle wheel suspension, the so-called “quarter vehicle” model, describing one of the four wheel is presented. It consists of a nonlinear system of three ordinary differential equations. During the vehicle’s motion the suspension reacts to the forces acting on it and, thus, influences the behavior of the whole car. The aim is to model this behavior and to investigate the conditions for quick and efficient damping of the resulting platform oscillations.

When a vehicle travels on a road, each of its suspensions is acted upon by the variations in the road profile, the input from the rest of the vehicle and the actuator. The model describes the dynamics of one of the suspensions. The road profile is represented by $R = R(t)$; the effect of the rest of the vehicle is denoted by $F_D = F_D(t)$ and the reaction of the a force actuator is described by $F_A = F_A(t)$. The case of a displacement actuator, which is easier to implement in practice, but more complicated theoretically, will be addressed in the near

future. The system, depicted in Fig. 2.1, can be represented by three masses m_1 , m_2 and m_3 connected with springs and dampers and an actuator for the platform control. Mass m_1 represents the wheel and the suspension itself; m_2 represents the part of the car above the wheel (“quarter vehicle”) including the driver and passengers; mass m_3 is small compared to the other two, and represents the active control mechanism.

The tire is characterized by the stiffness k_T and damping c_T ; the suspension by k_S and c_S ; the control mechanism by k_R . The nonlinear spring K_A , which forms the heart of the control system, is described below.

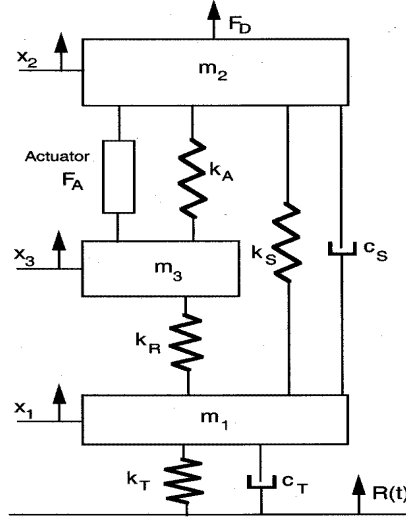


Figure 2.1: The setting

Let $x_1 = x_1(t)$, $x_2 = x_2(t)$ and $x_3 = x_3(t)$ be the respective displacements of the masses from their reference positions, positive when upward. Then, the motion of the system is described by the following system:

$$m_1 x_1'' = k_T(R - x_1) + c_T(R' - x_1') + k_S(x_2 - x_1) + c_S(x_2' - x_1') + k_R(x_3 - x_1), \quad (2.1)$$

$$m_2 x_2'' = k_S(x_1 - x_2) + c_S(x_1' - x_2') - K_A(x_3 - x_2) + F_D + F_A, \quad (2.2)$$

$$m_3 x_3'' = k_R(x_1 - x_3) + K_A(x_3 - x_2) - F_A. \quad (2.3)$$

Here, the prime indicates the time derivative. To complete the model the initial

conditions need to be prescribed,

$$x_1(0) = x_{10}, \quad x_2(0) = x_{20}, \quad x_3(0) = x_{30}, \quad (2.4)$$

$$x'_1(0) = v_{10}, \quad x'_2(0) = v_{20}, \quad x'_3(0) = v_{30}. \quad (2.5)$$

Here the x_{k0} are the initial positions and the v_{k0} the initial velocities, $k = 1, 2, 3$ of the masses.

The nonlinear element at the heart of the system is a spring which has a restoring force $K_A = K_A(x)$ that is depicted in Fig. 2.2. It is described by a curve which is decreasing on the interval $-\infty < x < g_1^*$, increasing on $g_1^* < x < g_2^*$, decreasing on $g_2^* < x < \infty$, and crossing the x -axis at $x = g_1, 0, g_2$; where $g_1 < g_1^* < 0 < g_2^* < g_2$. It is assumed below, for the sake of simplicity, that $-g_1 = g_2 = g$.

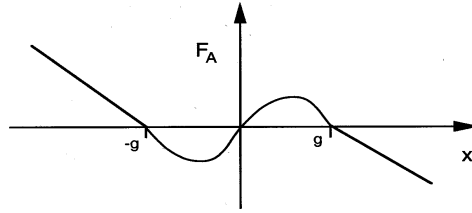


Figure 2.2: The restoring force K_A vs. displacement of the of the nonlinear spring.

A possible candidate with such behavior is the so-called “Duffing Oscillator,” which is characterizes by

$$K_A(x) = \alpha x - \beta x^3,$$

where α and β are positive constants.

Another device, the so-called Vertically Compressed Horizontally Sliding Spring (VCHSS), is obtained by a vertically positioned compressed spring the lower end of which may move on a horizontal rail, with

$$K_A(x) = -kx \left(1 - \frac{L_0}{\sqrt{x^2 + L^2}} \right).$$

Here, L_0 is the natural length of the spring, L is the compressed length and k is the spring constant. The spring is compressed in the vertical direction, while its lower end is restricted to move on a horizontal rail, and x is the horizontal distance from the origin. Clearly, for this choice of K_A the following relation

holds $g^2 + L^2 = L_0^2$. The details and analysis of such a system can be found in [6, 10].

The Bellville Washer is another example of a device with force-displacement characteristics depicted in Fig. 2.2. However, the load that it can support is too small to be of use in a car suspension mechanism.

The range $g_1 < x < g_2$ for which the spring deviates from a regular spring is determined by the suspension and system characteristics, and in practice has to be adjustable. The purpose is to have the operating range of the suspension within the interval $g_1 < x < g_2$, making it much easier to control and stabilize the system. However, since the system may have two stable steady states, in an actual suspension there is a need for an actuator F_A to guarantee that only one of them will be reached.

For a general spring K_A it is assumed that there exists a potential function $U_A = U_A(x)$ such that $U'_A = -K_A$, which acts as the potential energy of the spring. The form of U_A is depicted in Fig. 2.3. The potential energy of the Vertically Compressed Horizontally Sliding Spring is given by

$$U_A(x) = \frac{1}{2}k(x(t))^2 - kL_0\sqrt{(x(t))^2 + L^2} + k(L_0^2 - \frac{1}{2}g^2),$$

and it is scaled so that $U_A(g) = 0$, and then $0 \leq U_A$.

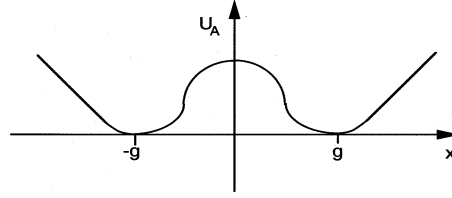


Figure 2.3: The potential energy U_A of the spring K_A .

When the VCHSS is considered on its own it exhibits three critical points. Two minimum points at $x = \pm g$ which are stable and one local maximum point at $x = 0$ which is unstable (see, e.g., [1, 13]).

Returning to the system (2.1)–(2.3) it is noted that since the nonlinear spring K_A is Lipschitz continuous, and the other right-hand sides are linear, the system has a unique local solution for each choice of the initial conditions (2.4) and (2.5) (cf., [8, 2]).

The system energy is considered next. The kinetic energy is

$$E_K(t) = \frac{1}{2}m_1(x'_1(t))^2 + \frac{1}{2}m_2(x'_2(t))^2 + \frac{1}{2}m_3(x'_3(t))^2, \quad (2.7)$$

and the potential energy is

$$E_P(t) = \frac{1}{2}k_T(x_1(t))^2 + \frac{1}{2}k_S(x_2(t) - x_1(t))^2 + \frac{1}{2}k_R(x_3(t) - x_1(t))^2 + U_A(x_3(t) - x_2(t)). \quad (2.8)$$

The total energy of the system is given by

$$E(t) = E_K(t) + E_P(t). \quad (2.9)$$

Consider now the system (2.1)–(2.5). Multiplying equation (2.1) by $x_1'(t)$, (2.2) by $x_2'(t)$, and (2.3) by $x_3'(t)$, integrating over $0 \leq s \leq t$ and adding up the resulting expressions, it follows, after integration by parts and rearranging, that

$$\begin{aligned} E(t) = & E(0) - c_T \int_0^t (x_1'(s))^2 ds - c_S \int_0^t (x_2'(s) - x_1'(s))^2 ds \\ & + \int_0^t (k_T R + c_T R') x_1'(s) ds + \int_0^t F_D x_2'(s) ds \\ & + \int_0^t F_A (x_2'(s) - x_3'(s)) ds. \end{aligned} \quad (2.10)$$

The two integrals with c_T and c_S represent the energy dissipated by the two dampers over the time interval $[0, t]$; the other three integrals on the right-hand side of (2.10) represent the energy input due to the work of external forces.

Consequently, when the system (2.1)–(2.5) is considered without external inputs, i.e., when $R = F_D = F_A = 0$, and without dissipation, i.e., $c_T = c_S = 0$, then the energy of the system is conserved. Thus,

$$E(t) = E(0),$$

for all $0 \leq t$. This estimate, in addition, guarantees that the system has a global solution, i.e., the solution exists on any time interval $[0, T]$. On the other hand, when the system includes dissipation but without external inputs, it follows from (2.10) that the energy is decreasing with time. The system, eventually, settles down at one of its steady states, which are discussed next.

Actually, it follows from (2.10) with zero inputs, $c_S = 0$ and $c_T > 0$ that

$$\frac{dE}{dt} = -c_T (x_1')^2,$$

that is, the system energy decays, and therefore so do the system oscillations. However, the rate of convergence of x_1, x_2 and x_3 to their steady states is left open.

3 Steady states

This section deals with the steady states of the system (2.1)–(2.3). As stated earlier, it is found that it may have either one or three steady states, depending on the system parameters.

To obtain the system steady states one sets the time derivatives in (2.1)–(2.3) equal zero. Assuming no external forces or inputs, we obtain

$$0 = -k_T \bar{x}_1 + k_S(\bar{x}_2 - \bar{x}_1) + k_R(\bar{x}_3 - \bar{x}_1), \quad (3.1)$$

$$0 = k_S(\bar{x}_1 - \bar{x}_2) - K_A(\bar{x}_3 - \bar{x}_2), \quad (3.2)$$

$$0 = k_R(\bar{x}_1 - \bar{x}_3) + K_A(\bar{x}_3 - \bar{x}_2). \quad (3.3)$$

Let η^* be a solution of the equation

$$\frac{k_R k_S}{k_R + k_S} \eta = K_A(\eta). \quad (3.4)$$

Then, each steady state satisfies,

$$\bar{x}_1 = 0, \quad (3.5)$$

$$\bar{x}_2 = -\frac{k_R}{k_S + k_R} \eta^*, \quad (3.6)$$

$$\bar{x}_3 = \frac{k_S}{k_S + k_R} \eta^*. \quad (3.7)$$

A graphic representation of the solutions of (3.4) is depicted in Fig. 3.1, where the slope of the line is given by

$$k^* = \frac{k_R k_S}{k_R + k_S},$$

which is positive.

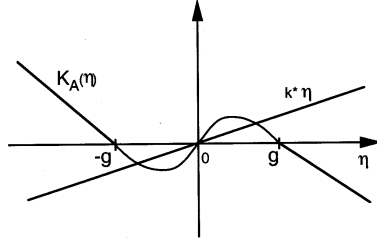


Figure 3.1: Equation (3.4) has three solutions.

It is noted that one of the roots must be $\eta^* = 0$ since both the straight line and the curve pass through the origin, and it is seen that when

$$\frac{k_R k_S}{k_R + k_S} > \max_{-g \leq \eta \leq g} |K'_A(\eta)|, \quad (3.8)$$

it is the unique solution, since the slope of the line on the left-hand side of (3.4) is greater than any slope of K_A for $-g \leq \eta \leq g$.

When the inequality in (3.8) is reversed there are three solutions as indicated in Fig. 3.1. The stability of these solutions is investigated numerically below. Based on these numerical simulations we conclude that when the root $\eta^* = 0$ is the unique solution of (3.4) it is stable. The other two roots, when existing, are stable, and then $\eta^* = 0$ is unstable. Thus, when

$$\frac{k_R k_S}{k_R + k_S} = K'_A(0),$$

i.e., when the line $k^* \eta$ is tangent to the curve $K_A(\eta)$ at the origin, bifurcation takes place, the root $\eta^* = 0$ loses its stability and two new stable solutions appear as the slope $K'_A(0)$ decreases through this value.

It might be of interest to investigate the behavior of the solutions as the bifurcation occurs, and also for large slopes of the straight line in Fig. 3.1. However, the main topic of this paper is the use of the system in the parameter range when there are three steady solutions, so that the origin is unstable.

4 Numerical simulations

In this section the numerical approach to the model is described and simulation results presented. The main goal of active suspension control is to provide comfort for the driver by having the motion $x_2(t)$ of m_2 damped and as even as possible, while having the wheel, m_1 following the road profile $R(t)$ as closely as possible, to provide the necessary traction with the road. However, as noted above, the actuator F_A which is needed in practice is not being used, and therefore, the simulations below describe the behavior of the system without any controls.

The Euler method is used for the time discretized approximation of the system. The time interval of interest is $[0, T]$, which is partitioned uniformly into N time steps $\Delta t = T/N$. Let $t_i = i\Delta t$ and let $x_l(i) = x_l(i\Delta t)$ denote the value of x_l at time t_i , for $l = 1, 2, 3$.

The second derivative of x_l at time t_i is approximated by

$$(x_l(t_i))'' = \frac{x_l(i) - 2x_l(i-1) + x_l(i-2)}{(\Delta t)^2}, \quad (4.1)$$

for $l = 1, 2, 3$, and $i = 0, 1, \dots, N$.

The only nonlinear term in the system, the force K_A , is given by

$$K_A(y) = k \left(1 - \frac{L_0}{\sqrt{y^2 + L^2}} \right) y.$$

It is approximated by retarding the argument one time step, thus,

$$K_A(y(i)) = k \left(1 - \frac{L_0}{\sqrt{y(i-1)^2 + L^2}} \right) y(i-1). \quad (4.3)$$

A somewhat different possible approximation is

$$K_A(y(i)) = k \left(1 - \frac{L_0}{\sqrt{y(i-1)^2 + L^2}} \right) y(i),$$

i.e., linearizing the expression. However, for the sake of simplicity (4.3) has been used, in the form

$$K_A(y(i)) = kM(y(i-1))y(i-1), \quad (4.4)$$

where

$$M(y(j)) = \left(1 - \frac{L_0}{\sqrt{y(j)^2 + L^2}} \right).$$

The following notation was used in the discretization of (2.1)–(2.3):

$$\begin{aligned} k_{T1} &= \frac{k_T}{m_1}, & k_{S1} &= \frac{k_S}{m_1}, & k_{R1} &= \frac{k_R}{m_1}, & k_{S2} &= \frac{k_S}{m_2}, & k_{R3} &= \frac{k_R}{m_3} \\ c_{T1} &= \frac{c_T}{m_1}, & c_{S1} &= \frac{c_S}{m_1}, & c_{S2} &= \frac{c_S}{m_2} \\ F_2 &= \frac{F_D + F_A}{m_2}, & F_3 &= \frac{F_A}{m_3}. \end{aligned}$$

Next, let

$$\begin{aligned} \alpha_1 &= 1 + (\Delta t)^2(k_{T1} + k_{S1} + k_{R1}) + (\Delta t)(c_{T1} + c_{S1}), \\ \alpha_2 &= 1 + (\Delta t)^2k_{S2} + (\Delta t)c_{S2}, \\ \alpha_3 &= 1 + (\Delta t)^2k_{R3}. \end{aligned}$$

Using the approximations (4.1), (4.3) and the notation above in the system (2.1)–(2.3) yields the following discretized system for $\{x_1(i), x_2(i), x_3(i)\}$, at time $t_i = i\Delta t$,

$$\begin{aligned} \alpha_1 x_1(i) &= (2 + (\Delta t)(c_{T1} + c_{S1}))x_1(i-1) - x_1(i-2) + k_{S1}(\Delta t)^2 x_2(i-1) \\ &\quad + k_{R1}(\Delta t)^2 x_3(i-1) + c_{S1}(\Delta t)(x_2(i-1) - x_2(i-2)) \\ &\quad + (\Delta t)^2(k_{T1}R + c_{T1}R'), \end{aligned} \quad (4.5)$$

$$\begin{aligned} \alpha_2 x_2(i) &= (2 + (\Delta t)c_{S2})x_2(i-1) - x_2(i-2) + k_{S2}(\Delta t)^2 x_1(i) \\ &\quad + c_{S2}(\Delta t)(x_1(i) - x_1(i-1)) + (\Delta t)^2 F_2 \\ &\quad - \frac{k(\Delta t)^2}{m_2} M(x_3(i-1) - x_2(i-1))(x_3(i-1) - x_2(i-1)) \end{aligned} \quad (4.6)$$

$$\begin{aligned} \alpha_3 x_3(i) &= 2x_3(i-1) - x_3(i-2) + k_{R3}(\Delta t)^2 x_1(i) - (\Delta t)^2 F_3 \\ &\quad + \frac{k(\Delta t)^2}{m_3} M(x_3(i-1) - x_2(i-1))(x_3(i-1) - x_2(i-1)) \end{aligned} \quad (4.7)$$

The numerical algorithm proceeds as follows: Starting with the initial conditions (2.4) and (2.5), if the solution $\{x_1(j), x_2(j), x_3(j)\}$, for $j = 0, 1, \dots, i-1$,

i.e., up to the time $t = (i - 1)\Delta t$ is known, then $\{x_1(i), x_2(i), x_3(i)\}$ are computed at time step i , using (4.5)–(4.7). Then the algorithm marches to the time step $i + 1$, for $i = 2, 3, \dots, N$. After each time step, the values are updated, and the next time step computed.

The numerical simulations are described next. Four simulations are presented: an initial entry of the driver into the car and a flat road; a wavy (periodic) road, a bump on a flat road; a bump on a periodic road. The aim is to present typical types of behavior of the system. However, the phase space is six-dimensional so the more interesting graphs in each example are presented, such as the time evolution of one of the variables or the two-dimensional cross section of the phase space, the phase-plane.

The system is very interesting and warrants further simulations and analysis.

The values of the coefficients used in the simulations were $k_T = 180,000$, $k_S = 30,000$, $k_R = 400,000$ [n/m], $m_1 = 50$, $m_2 = 400$, $m_3 = 5$ [kg], and $c_t = c_S = 10$ [$n \cdot sec/m$].

The road profile was described by the function $R = R(t)$ [m], with time derivative R' . The initial conditions for x_1 , which is directly related to the road profile, and x_2 which is related to the driver, are specified in the examples, while the rest of the initial conditions were chosen as $x_3(0) = \dot{x}_3(0) = 0$ in all four examples.

In the VCHSS (4.3), the following values of the constants were employed: $k = 20,000$ [n/m] and $L = 4$, $L_0 = 6$ [m]. This choice is not particularly useful in a car, and was made for the sake of clear illustrations of the behavior, since it made the two stable equilibrium positions close to each other.

The simulation code was written in Maple 6, and a typical run of 8,000 time steps took about 40 [sec], on the 450Mhz Power Mac G4 machine.

The simulations results are described now.

4.1 Example 1- Flat road with initial displacement

The first example describes the case of an initial disturbance, say when a passenger leaves the car. The initial conditions chosen were $x_1(0) = \dot{x}_1(0) = 0$ and $x_2(0) = 0.1$, $\dot{x}_2(0) = -0.1$, while the road was flat, i.e., $R(t) = 0$. The time step was $\Delta t = 0.005$, and it was found that qualitatively changing the time step produced similar results. However, the system is sensitive to initial conditions and small changes in them may lead the system trajectory to switch from one steady state to the other.

The displacements of the wheel and suspension x_1 and of the car and passengers mass x_2 , as functions of time, are depicted in Fig. 4.1 and the evolution of the nonlinear spring x_3 in Fig. 4.2, as well as the trajectory in the phase plane $x_3 - \dot{x}_3$. It is seen that the initial oscillation dissipated rather quickly, in 20 seconds or so, although, as noted above, the system was very lightly damped. Then it settled in one of its steady states. It is noted that the origin was repulsive.

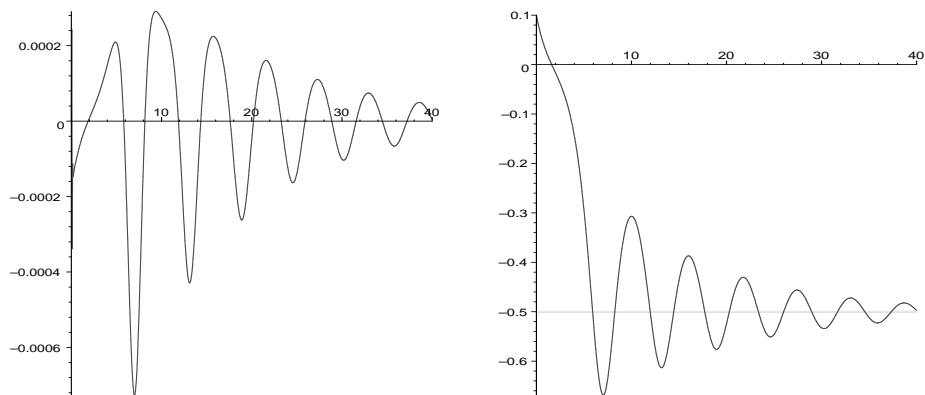


Figure 4.1: Example 1: evolution of x_1 and x_2

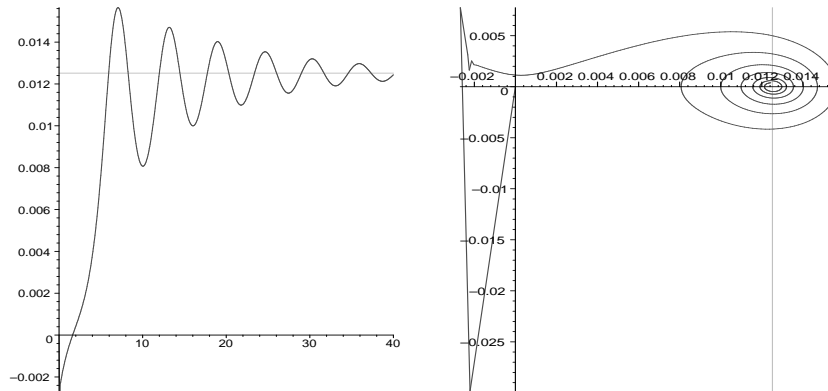


Figure 4.2: Example 1: evolution of x_3 and the $x_3 - \dot{x}_3$ -plane

4.2 Example 2- Periodic road

The road was assumed periodic with profile $R(t) = A \cos(\omega t)$, with frequency $\omega = 10$, i.e. $5/\pi$ [hertz], and amplitude $A = 0.1$ [m]. The initial conditions were $x_1(0) = \dot{x}_1(0) = x_2(0) = \dot{x}_2(0) = 0$. The time step used was $\Delta t = 0.005$.

The displacements of the wheel and suspension x_1 were found to follow R very closely. The displacements x_2 and the phase plane $x_2 - \dot{x}_2$ are depicted in Fig. 4.3, where it is seen that $x - 2$ settles very quickly into a periodic motion with the same period as the road's. The evolution of x_3 and the phase plane $x_3 - \dot{x}_3$ are depicted in Fig. 4.4. Within 20 seconds or so, the system settles into a periodic oscillation about the upper equilibrium position, following the road. The transition to periodic oscillations can be clearly seen in Fig. 4.4.

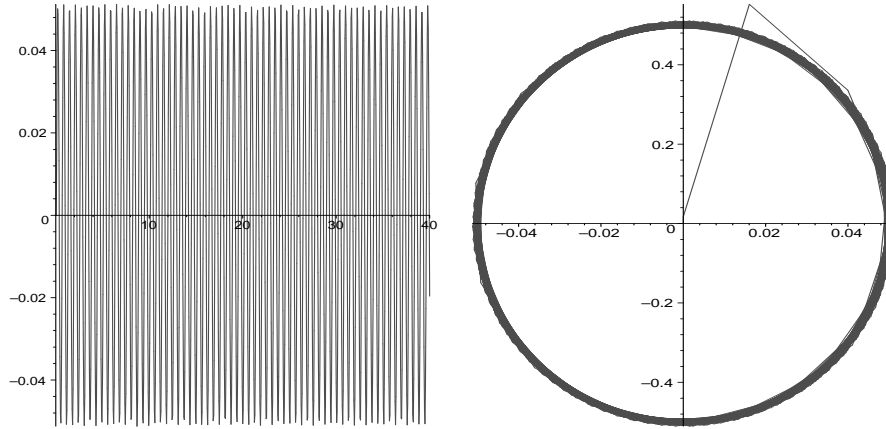


Figure 4.3: Example 2: evolution of x_1 and the phase plane $x_1 - \dot{x}_1$

4.3 Example 3- Bump in the road

A road bump was considered, in the form depicted in Fig. 4.5, with amplitude 0.15 [m]. The initial conditions were $x_1(0) = \dot{x}_1(0) = x_2(0) = \dot{x}_2(0) = 0$. The time step used was $\Delta t = 0.005$.

The decay of the induced oscillations and approach to the steady state can be seen clearly in Fig. 4.6. The phase plane $x_3 - \dot{x}_3$ is shown in Fig. 4.7.

4.4 Example 4- Bump in a periodic road

In addition to a periodic road profile, a road bump was added, thus combining the effects of the two examples above. Since the system is nonlinear, it is seen that the effects are not additive.

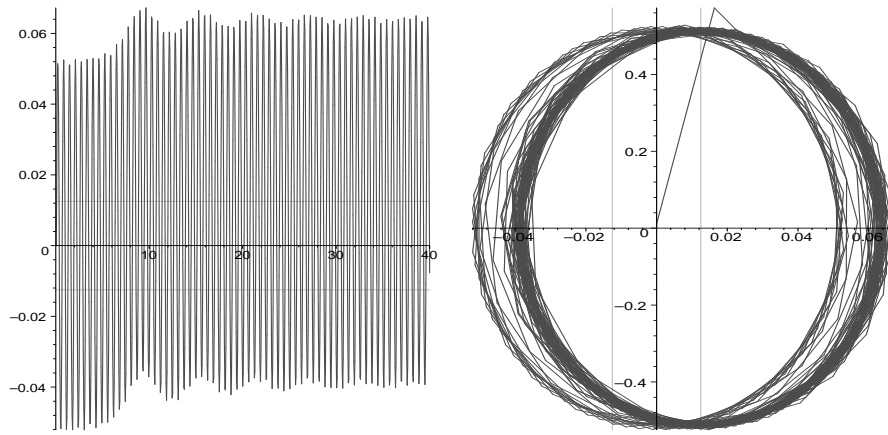


Figure 4.4: Example 2: evolution of x_3 and the phase plane $x_3 - \dot{x}_3$

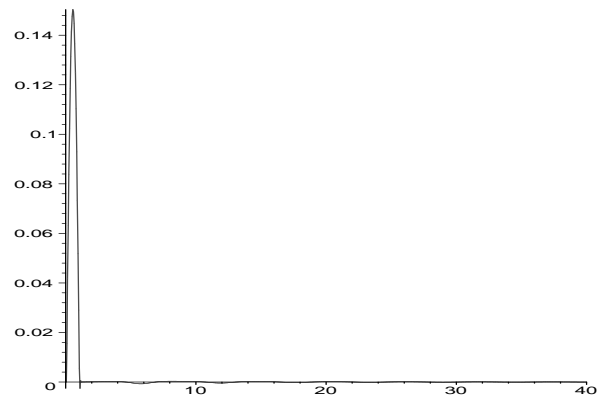


Figure 4.5: Example 3: evolution of x_1

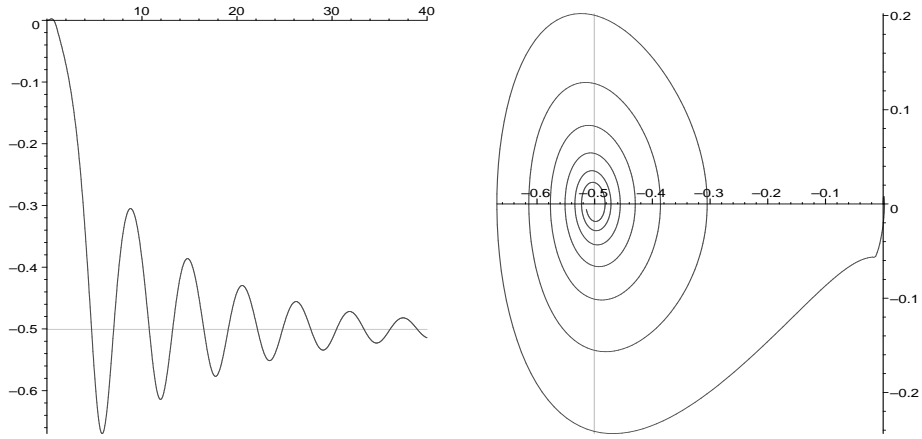


Figure 4.6: Example 3: evolution of x_2 and the phase plane $x_2 - \dot{x}_2$

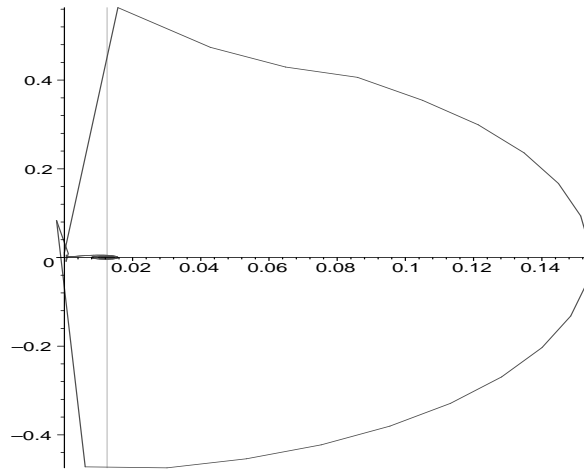


Figure 4.7: Example 3: the phase plane $x_3 - \dot{x}_3$

A road bump was the same as in Example 3, in the form depicted in Fig. 4.5, with amplitude $0.15[m]$. The road profile was the same as in Example 2, $R(t) = A \cos(\omega t)$, with frequency $5/\pi[hertz]$, and amplitude $A = 0.1[m]$. The initial conditions were $x_1(0) = \dot{x}_1(0) = x_2(0) = \dot{x}_2(0) = 0$. The time step used was $\Delta t = 0.005$.

Since the problem is nonlinear the effects are not additive. However, the system settles quickly into the behavior in the periodic case.

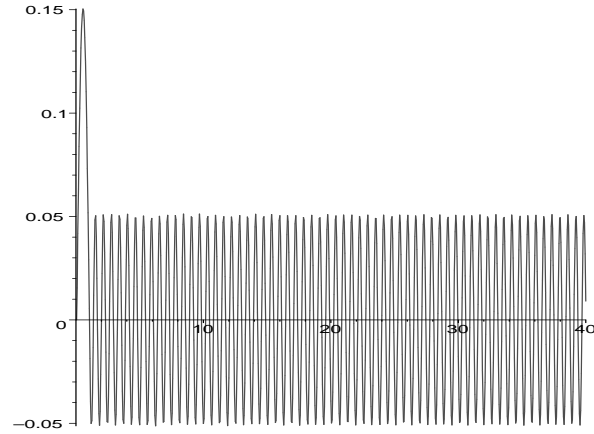


Figure 4.8: Example 4: evolution of x_1

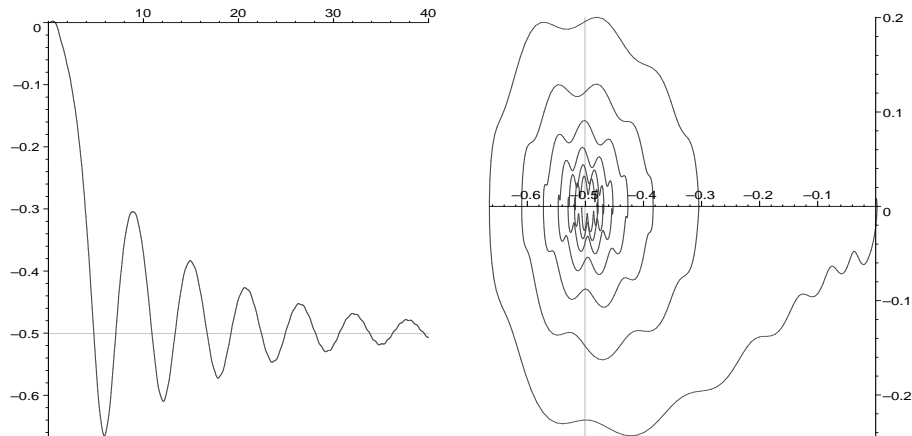


Figure 4.9: Example 4: evolution of x_2 and the phase plane $x_2 - \dot{x}_2$

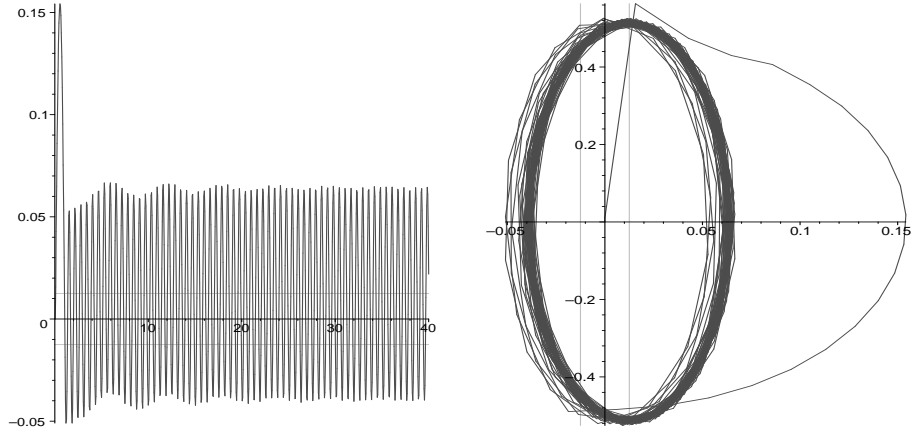


Figure 4.10: Example 4: evolution of x_3 and the phase plane $x_3 - \dot{x}_3$

5 Conclusions

A novel system for the stabilization of automotive platform has been presented. It is in the form of a nonlinear system of ordinary differential equations. The main element in the system is a nonlinear spring with a negative spring constant over the relevant range of its displacements. The energy of the system was shown to be conserved or to decay, depending on the presence of damping. The system can have either one or three steady states, and the numerical simulations indicate, as expected, that the zero solution is stable when unique and unstable when the other two solutions are stable. Moreover, the solutions converge quickly to one of the stable steady states.

The system, without the control actuator is of some interest in its own right, in showing that the system stabilizes very quickly with small damping. However, without the actuator, the system may jump between the two stable steady states. Therefore, a displacement actuator is needed, and the resulting problem will be investigated in the near future. Moreover, by employing a displacement actuator, the character of the model changes and instead of a system of ODEs the model consists of inequalities or set-inclusions.

A numerical scheme for the problem was described and the results of numerical simulations presented. It was shown that the system may behave in interesting ways, and further numerical and mathematical investigation of this model is in order.

References

- [1] J. Argyris, G. Faust and M. Haase, *An Exploration of Chaos*, Elsevier Science, Amsterdam 1994.

- [2] V. I. Arnold, *Ordinary Differential Equations*, MIT Press, Cambridge, 1973.
- [3] D. S. Cameron and N. Kheir, *On the modeling of ground vehicle control*, Proc. 35th Conference on Decision and Control, Kobe, Japan, December 1996, pp. 3570–3574.
- [4] D. S. Cameron and N. Kheir, *Ground vehicle suspensions: Categorization, classification and a proposed novel active suspension system*, Intl. Federation of Information Processing Conference, Detroit, USA, 1997, presented.
- [5] D. S. Cameron, N. Kheir and M. Shillor, *Low energy active platform stabilizing suspension system*, preprint.
- [6] D. S. Cameron, *Platform stabilization with a novel active suspension*, Ph.D. Thesis, Department of Electrical Engineering, Oakland University, 1999.
- [7] J. Darling, R. E. Dorey and T. J. Ross-Martin, *A low cost active anti-roll suspension for passenger cars*, Transactions of the ASME J. Dynamic Systems, Measurements and Control, **114**(3)(1992), 599–605.
- [8] E. A. Coddington and N. Levinson, *Theory of Ordinary Differential Equations*, McGraw-Hill, New York, 1955.
- [9] J. Dominy and D. N. Bulman, *An active suspension for a Formula One Grand Prix racing car*, Transactions of the ASME J. Dynamic Systems, Measurements and Control, **107**(March 1985), 73–78.
- [10] Y. Dumont, D. Goeleven, M. Rochdi and M. Shillor, *Frictional contact of a nonlinear spring*, Math. Computer Modelling, **31**(2000), 83–97.
- [11] D. Hrovat, D. L. Margolis and M. Hubbard, *An approach toward the optimal semi-active suspension*, Transactions of the ASME J. Dynamic Systems, Measurements and Control, **110**(September 1988), 288–296.
- [12] P. J. Th. Venhovens, A. C. M. Van der Knapp and H. B. Pacejka, *Semi-active attitude and vibration control*, Intl. J. Vehicle Mech. Mob., Vehicle System Dynamics, **22**(1993), 359 – 381.
- [13] S. Wiggins, “Introduction to Applied Dynamical Systems and Chaos,” Springer, New York, 1990.